Gamma-Secretase Complexes Regulate the Responses of Human Pancreatic Ductal Adenocarcinoma Cells to Taxanes

TAKEHIKO TASAKA[1], TAKASHI AKIYOSHI[2], KOJI YAMAGUCHI[3], MASAO TANAKA[4], HIDEYA ONISHI[1] and MITSUO KATANO[1]

Departments of [1]Cancer Therapy and Research, and [4]Surgery and Oncology, Graduate School of Medical Sciences, Kyushu University, Fukuoka 812-8582, Japan; [2]Gastroenterological Center, Department of Gastroenterological Surgery, Cancer Institute Ariake Hospital, 3-10-6 Ariake, Koto-ku, Tokyo 135-8550, Japan; [3]Department of Surgery 1, School of Medicine, University of Occupational and Environmental Health, Kitakyushu 807-8555, Japan

Abstract. *Background/Aim: It was previously reported that γ-secretase inhibitors (GSIs) enhance taxane-induced mitotic arrest and apoptosis in colon cancer cells. To enable the development of taxane-based chemotherapy for pancreatic ductal adenocarcinoma (PDAC), this study investigated the molecular mechanisms by which γ-secretase (GS) complexes regulate taxane sensitivity. Materials and Methods: The effect of GS complexes on taxane-induced apoptosis in PDAC cells was evaluated by a cell cycle analysis. GS complexes were examined with small interference RNAs targeted to GS complex-related genes. Results: GSIs and silencing of presenilin 1 (PS1) did not affect cell proliferation but resulted in enhanced taxane-induced G_2/M accumulation and apoptosis. Silencing of the Notch gene did not induce these effects. However, PS2-specific silencing suppressed proliferation and taxane-induced apoptosis. Conclusion: Data from this study indicate that GS complexes regulate the response of PDAC to taxanes through GS-dependent and GS-independent mechanisms.*

Pancreatic ductal adenocarcinoma (PDAC) is one of the most deadly types of cancer (1). It was previously reported that γ-secretase inhibitors (GSIs) enhance taxane-induced apoptosis in colon cancer cells (2). Therefore, it was hypothesised that combined taxane and GSI treatment may be an effective strategy against taxane-resistant cancer, including PDAC. Furthermore, the effect of GSIs in PDAC cells was confirmed in the current study. Therefore, to examine the clinical application of GSIs for incurable PDAC, we analysed the molecular mechanisms involved in the enhancement of taxane-induced apoptosis by GSI treatment.

γ-Secretase (GS) complexes are multi-subunit aspartyl proteases, consisting of 4 proteins: presenilin (PS), nicastrin (NCT), anterior pharynx defective-1 (Aph-1), and presenilin enhancer 2 (Pen2) in equal quantities (3). There are two homologues of PS (PS1 and PS2), and three isoforms of Aph-1 (Aph-1aS, Aph-1aL, and Aph-1b). Because GS complexes contain only one of each subunit (3), at least six active GS complexes have been reported (two PSs × three Aph-1s) (4). Although the catalytic core of the GS complex exists in PS, the cleavage of substrates by GS requires a free *N*-terminal amine (5). NCT can only recruit substrates that have a free *N*-terminal amine in which their large extracellular domains are already removed by a proteinase in a process termed 'ectodermal shedding'. NCT therefore functions as a receptor for GS substrates. However, to display full GS activity, PS must be endoproteolytically cleaved into an *N*-terminal fragment (PS-NTF) and a *C*-terminal fragment (PS-CTF), each of which contains an active-site aspartate residue. It has been proposed that NCT and Aph-1 forms an initial complex in GS complexes, and Aph-1 and NCT are therefore believed to be responsible for the formation of GS complexes. Taken together, all four proteins are necessary and sufficient for GS activity (6). Although both PS1 and PS2 are essential for GS-mediated cleavage, the dramatically different phenotypes of the PS1-deficient and PS2-deficient mice suggest disparate roles of these proteins (7). PS1-deficient mice exhibit severe developmental defects and perinatal lethality (8), whereas

Correspondence to: Mitsuo Katano, Department of Cancer Therapy and Research, Graduate School of Medical Sciences, Kyushu University, 3-1-1 Maidashi, Higashi-ku, Fukuoka 812-8582, Japan. Tel: +81 926426219, Fax: +81 926426221, e-mail: mkatano@tumor.med.kyushu-u.ac.jp

Key Words: Apoptosis, presenilin 1, presenilin 2, cell cycle, G_0/G_1, chemoresistance, γ-secretase, pancreatic ductal adenocarcinoma cells, taxanes.

PS2-deficient mice are viable and fertile (7). In addition, it has been shown that GS complexes have GS activity-independent biological functions (9).

GS substrate candidates are increasing in number, and there are over 25 substrates to date, including amyloid β (Aβ)-peptide, Notch, E-cadherin, and CD44 (10). Among these proteins, it has been shown that Notch signalling plays a central role in cell fate during embryonic development of the pancreas, and that Notch signalling is frequently dysregulated in several types of cancer including PDAC (11). Binding of ligands to Notch receptors results in GS-induced proteolytic cleavage of the transmembrane part of Notch, releasing the Notch intracellular domain (NICD) (12). NICD translocates to the nucleus and interacts with the ubiquitous transcription factor CBF1, thereby activating transcription (13). Therefore, GSIs are expected to be potential novel cancer therapeutic agents (14). GSIs are classified into three types, based on the site of GS binding: active site-binding GSIs, substrate docking site-binding GSIs, and alternative binding site GSIs (15). *N*-[*N*-(3,5-Difluorophenacetyl-L-alanyl)]-*S*-phenylglycine *t*-butyl ester (DAPT) is an alternative binding site-based GSI and binds to PS-CTF (15). {1S-Benzyl-4R-[1-(1S-carbamoyl-2-phenethylcarbamoyl)-1S-3-methylbutylcarbamoyl]-2R-hydroxy-5-phenylpentyl} carbamic acid *tert*-butyl ester (L-685,458) is an active site-binding GSI and binds to PS-NTF (15).

(S,S)-2-[2-(3,5-Difluorophenyl)-acetylamino]-*N*-(1-methyl-2-oxo-5-phenyl-2,3-dihydro-1H-benzo[e][1,4]diazepin-3-yl)-propionamide (compound E), is a miscellaneous GSI and binds to PS-NTF (16). However, a recent study has shown that the specificity of PS1 and PS2 toward identical substrates is different, and that GSIs exhibit different activities toward PS1-GS compared to PS2-GS (17).

Microtubules are highly dynamic cytoskeletal fibres that are composed of α- and β-tubulin subunits and play a crucial role in mitosis and cell division (18). Taxanes, including paclitaxel (TXL) and docetaxel (TXT), bind to β-tubulin on the inside microtubule surface, stabilise the microtubule, and increase microtubule polymerisation (19). As a result, taxanes halt cell cycle progression in the late G_2/M phase through the prevention of mitotic spindle formation (19). To progress from the G_2 phase to the M phase, cells must pass through the G_2/M checkpoint (20). CDC2, the cyclin-dependent kinase that normally drives cells into mitosis, is the ultimate target of pathways that mediate rapid arrest in G_2 phase in response to DNA damage (21). Cyclin A and B, which bind to CDC2, accumulate as the cell progresses through the G_2 phase (21). During the G_2 phase, the CDC2/cyclin B1 complex is sequestered in the cytoplasm (21). As cells approach the G_2/M boundary, cyclin B1 becomes phosphorylated and the CDC2/cyclin B complex accumulates in the nucleus, where it can induce entry into mitosis (21). Therefore, CDC2 is an important effector for the G_2/M checkpoint (21). Although taxane-induced apoptosis appears to occur following a prior mitotic arrest, it has been shown that the low concentration of taxanes used in this study causes G_2/M accumulation and apoptosis in the absence of mitotic arrest (22). A high concentration of taxanes may therefore induce mitotic arrest without an increase in apoptosis, and a low concentration of TXL may increase apoptosis without an increased mitotic arrest. Therefore, apoptosis and mitotic arrest can occur independently, and different phenotypes induced by TXL may be concentration dependent.

This study reports that inhibition of PS-GS enhances taxane-induced apoptosis of PDAC cells. In addition, this effect is not dependent on Notch signalling. Significantly, the present study is the first demonstrating that PS, and PS2 in particular, controls cell cycle progression in a GS-independent manner. GS complexes may regulate the response of PDAC cells to anti-microtubule agents (AMAs) through both GS-dependent and GS-independent mechanisms. The Authors believe that these novel findings enable the development of GS complexes-targeted strategies for the treatment of patients with highly chemoresistant PDAC.

Materials and Methods

Reagents and cell cultures. TXL, TXT, vincristine (VCR) and 5-fluorouracil (5-FU) were obtained from Sigma-Aldrich (St Louis, MO, USA). Gemcitabine (GEM) and cisplatin (CDDP) were obtained from LKT Laboratories (St. Paul, MN, USA). GSIs (DAPT, L-685,458, and compound E), and the cdk inhibitor (2-(R)-(1-ethyl-2-hydroxyethylamino)-6-benzylamino-9-isopropylpurine, Roscovitine) were obtained from Calbiochem (San Diego, CA, USA). Five PDAC cell lines were used. AsPC-1, SUIT-2, PANC-1, and CFPAC-1 were maintained in RPMI-1640 medium (Nacalai Tesque, Kyoto, Japan) supplemented with 10% foetal bovine serum (FBS: Biological Industries, Kibbutz Beit Haemek, Israel), at 37˚C in 5% CO_2. MIAPaCa-2 was maintained in DMEM (Invitrogen Carlsbad, CA, USA) supplemented with 10% FBS at 37˚C in 5% CO_2. Human umbilical vein endothelial cells (HUVECs) were maintained in EBM-2 medium (Lonza Walkersville, Inc., USA) supplemented with EGM-2 SingleQuots (Lonza), at 37˚C in 5% CO_2.

Flow cytometry. Cells (3.2×10^5 cells/well) were plated in 6-well plates, and treated with the appropriate combinations of drugs. Adherent and detached cells were harvested by trypsinization, and fixed in ice-cold 75% ethanol for at least one hour. Cell pellets were washed twice with cold phosphate-buffered saline (PBS), and incubated for 30 min at room temperature in 1 ml PBS containing 50 μg propidium iodide (Sigma-Aldrich), 0.1% Triton X-100, 1 mM/l EDTA, and 0.5 mg ribonuclease A. After staining, samples were analysed using FACScan (BD Biosciences, San Jose, CA, USA) at 20,000 events per sample. Data from flow cytometry were analysed with the ModFit LT software program (Verity Software House, Topsham, ME, USA). Fragmented apoptotic nuclei were recognisable by their subdiploid (sub-G_1) DNA content. The percentage of sub-G_1 cells was recorded for each sample.

RNA interference. Small interfering RNAs (siRNAs) for *Notch1* (ON-TARGET*plus* SMART pool L-007771), *Notch2* (ON-

Table I. *Sequences of primers used in this study.*

Primers for RT-PCR		
Target	Forward primer	Reverse primer
Notch1	5'-GCCGCCTTTGTGCTTCTGTTC-3'	5'-CCGGTGGTCTCTCTGGTCGTC-3'
Notch2	5'-CACTGAGCCAAGGCATAGAC-3'	5'-ATCTGGAAGACACCTTGGGC-3'
Notch3	5'-TCTTGCTGCTGGTCATTCTC-3'	5'-TGCCTCATCCTCTTCAGTTG-3'
Notch4	5'-CACTGGGTCGATGATGAAGG-3'	5'-ATCTCCACCTCACACCACTG-3'
β-actin	5'-CCAGGCACCAGGGCGTGATG-3'	5'-CGGCCAGCCAGGTCCAGACG-3'
Primers for real-time RT-PCR		
Target	Forward primer	Reverse primer
Notch1	5'-CCGCAGTTGTGCTCCTGAA-3'	5'-ACCTTGGCGGTCTCGTAGCT-3'
Notch2	5'-CACCATGTACCAGATTCCAG-3'	5'-GCATAACTGTGCTGTGAAGG-3'
Notch3	5'-TCTCAGACTGGTCCGAATCCAC-3'	5'-CCAAGATCTAAGAACTGACGAGCG-3'
RBPSUH	5'-GCAATGCTTGAACTTACAGGACAGA-3'	5'-TTCCATCATTTCGGACCAAAGTTAC-3'
PSEN1	5'-TGAGGGTTTCAGTGGGATCATTTAC-3	5'-CAAAGCAGTGTCCACAGAAGCAG-3'
PSEN2	5'-TGCTCTACAAGTACCGCTGCTACAA-3'	5'-ATGCACACCATGCCCACTG-3'
NCSTN	5'-GAGCAGTGCCAGGATCCAAGTAA-3'	5'-CCCTGGCTAATCGTGCAGTAGAA-3'
CDC2	5'-GAAGTGTGGCCAGAAGTGGAATC-3'	5'-CCAGAAATTCGTTTGGCTGGA-3'
CCNB1	5'-AATGAAATTCAGGTTGTTGCAGGAG-3'	5'-CATGGCAGTGACACCAACCAG-3'
CCND1	5'-ACAAACAGATCATCCGCAAACAC-3'	5'-TGTTGGGGCTCCTCAGGTTC-3'
MYC	5'-CAGCTGCTTAGACGCTGGATT-3	5'-GTAGAAATACGGCTGCACCGA-3'
β-actin	5'-CCAGGCACCAGGGCGTGATG-3'	5'-CGGCCAGCCAGGTCCAGACG-3'

TARGET*plus* SMART pool L-012235), *Notch3* (ON-TARGET*plus* SMART pool L-011093), *RBPSUH* (gene encoding CBF1, ON-TARGET*plus* SMART pool L-007772), *NCTSN* (gene encoding Nicastrin ON-TARGET*plus* SMART pool L-008043), *CCNB1* (gene encoding cyclin B1, ON-TARGET*plus* SMART pool L-003206) and negative control siRNA (ON-TARGET*plus* SMART pool D-001810) were obtained from Dharmacon RNA Technologies (Chicago, IL, USA). siRNAs against *PSEN1* (Stealth Select RNAi HSS108649), *PSEN2* (Stealth Select RNAi HSS108653), *CDC2* (gene encoding cdk1, Validated Stealth RNAi Duplex1, 12935-006) and Stealth RNAi Negative Control were obtained from Invitrogen. Cells were transfected with 50 nM siRNA using the Lipofectamine RNAiMAX Reagent (Invitrogen) according to the manufacturer's instructions. At 48 h after transfection, cells were harvested and subjected to further analyses.

Plasmids and cell transfection. pCS2$^+$ and pCS2$^+$NICD were kindly provided by Dr. Raphael Kopan (Washington University, USA). Cells were plated onto 12-well plates 24 h before transfection, and transfected with TransFast Transfection Reagent (Promega, Madison, WI, USA) according to the manufacturer's instructions.

Proliferation assay. Cells (5×10^3 cells/well) were seeded into 48-well plates in complete culture medium and were incubated for 24 h at 37˚C. The medium was changed and treated with the appropriate concentrations of drugs. After 48, 72 or 96 h, cells were harvested and counted using a particle size distribution analyser (CDA-500; Sysmex, Hyogo, Japan). Each sample was run in triplicate.

Hoechst 33342 staining. Apoptotic cells were assessed for nuclear changes (*i.e.* chromatin condensation and nuclear fragmentation) characteristic of apoptosis using Hoechst 33342 dye (Sigma-Aldrich). In brief, cells were grown in 6-well plates and stained with Hoechst 33342 dye. Cells were examined by fluorescence microscopy. The numbers of apoptotic nuclei in five randomly selected fields (objective lens, ×200) were counted, and apoptosis was expressed as the percentage of cells with apoptotic characteristics compared to the total number of cells examined.

Reverse-transcription polymerase chain reaction (RT-PCR). Total RNA was isolated with the High Pure RNA Isolation Kit (Roche Diagnostics GmbH, Mannheim, Germany). Complementary DNA (cDNA) was synthesised by reverse transcribing total RNA with ImProm-II Reverse Transcriptase (Promega). Standard PCR reactions were performed using the HotStarTaq DNA polymerase (Qiagen, Valencia, CA, USA). The sequences of primers used are listed in Table I.

Real-time RT-PCR. Total RNA was reverse transcribed using the Quantitect Reverse Transcription Kit (Qiagen) according to the manufacturer's protocol. Reactions were performed with SYBR Premix Ex Taq II (Takara Bio, Shiga, Japan) on a DNA Engine Opticon 2 system (MJ Research, Waltham, MA, USA). Each sample was run in triplicate. The sequences of primers used are listed in Table I.

Immunoblotting. Whole-cell protein extracts were isolated with the M-PER Mammalian Protein Extraction Reagent kit (Thermo Fisher Scientific, Rockford, IL, USA) according to the manufacturer's instructions. Whole-cell protein extract (75 μg) was separated by

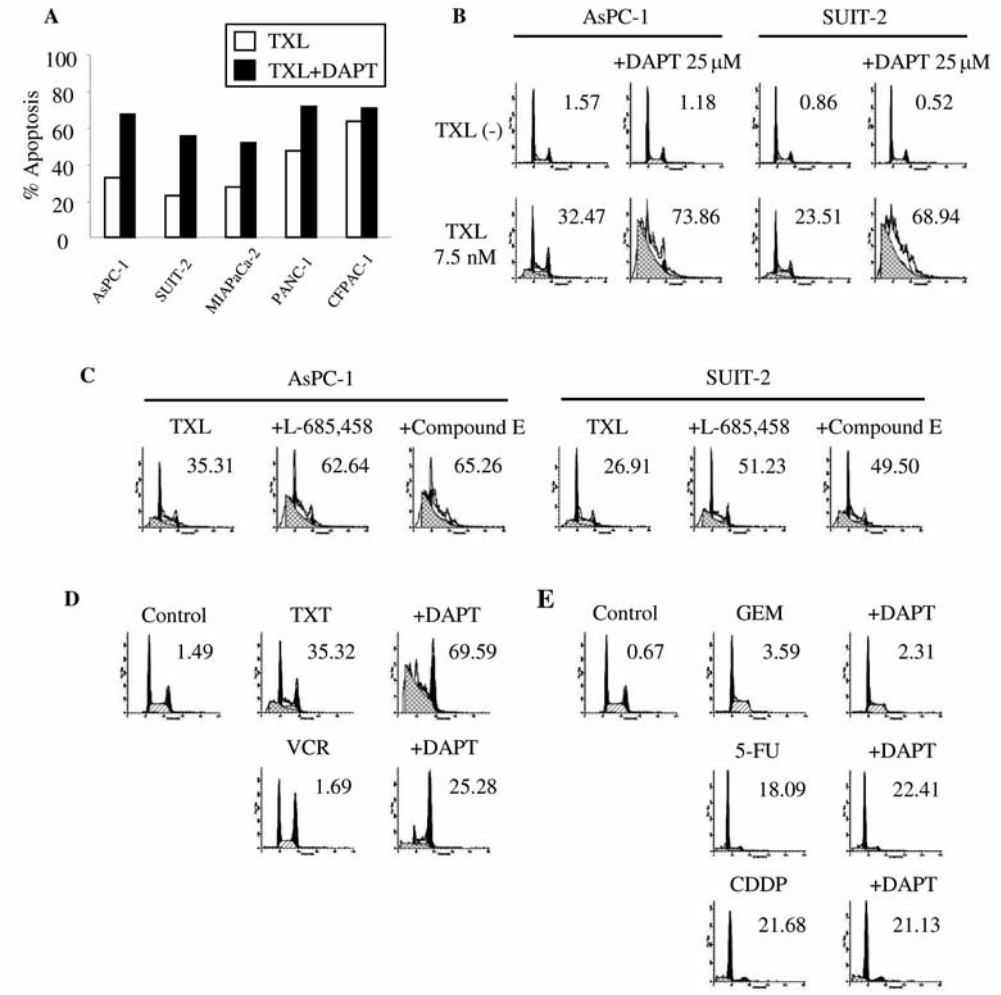

Figure 1. *Increased TXL-induced apoptosis by treatment with GSIs is dependent on GS activity. A: DAPT increases TXL-induced apoptosis. Five PDAC cell lines were treated with the indicated TXL concentrations for 24 h in the absence or presence of 25 μM DAPT. Cells were then stained with Hoechst 33342 and examined by fluorescence microscopy. Apoptotic cells were quantified. B: AsPC-1 and SUIT-2 cells were treated with 7.5 nM TXL in the absence or presence of 25 μM DAPT for 24 h, and the cell cycle was analysed by flow cytometry. The percentage of sub-G_1cells is indicated. C: Cells were treated with 7.5 nM TXL in the absence or presence of 5 μM L-685,458 or 10 μM compound E for 24 h. The percentage of sub-G_1 cells is indicated. D: AsPC-1 cells were treated with 8 nM TXT or 100 nM VCR in the absence or presence of 25 μM DAPT for 24 h. The percentage of sub-G_1 cells is indicated. E: AsPC-1 cells were treated with 200 nM GEM, 300 μg/ml 5-FU or 80 μM CDDP in the absence or presence of 25 μM DAPT for 24 h. The percentage of sub-G_1 cells is indicated.*

electrophoresis on a 7.5% SDS-polyacrylamide gel and electro-transferred to nitrocellulose membranes. Anti-Notch1 (1:200, C-20; Santa Cruz Biotechnology, CA, USA), anti-Notch2 (1:200, C651.6DbHN originally developed by Dr Artavanis-Tsakonas and obtained from the University of Iowa Development Hybridoma Studies Bank, USA), anti-Notch3 (1:200, M-20; Santa Cruz Biotechnology) and anti-β-actin (1:500, I-19; Santa Cruz Biotechnology) antibodies were used as primary antibodies. After washing, membranes were incubated with the appropriate horseradish peroxidase-conjugated secondary antibody (GE Healthcare UK Ltd., UK). Blots were developed using the ECL Plus Western Blotting Detection System (GE Healthcare).

Immunofluorescence staining. Cells (2×10^4 cells/well) were seeded onto pre-underlaid poly-L-lysine coated glass coverslips (Asahi Techno Glass Corporation, Chiba, Japan) in 24-well plates, and were incubated for 24 h in complete culture medium. The cells were fixed in 4% paraformaldehyde and incubated with the primary antibody, followed by the secondary antibody. The cells were counterstained with 4',6-diamino-2-phenylindole (DAPI; Sigma-Aldrich) to visualise the nuclei. After mounting in Vectorshield Mounting Medium (Vector Laboratories, Burlingame, CA, USA), the samples were examined by fluorescence microscopy (Axiomager A1; Carl Zeiss Imaging, Tokyo, Japan). The antibodies and dilutions used were as follows: anti-PS1 (1:100, C-20; Santa Cruz Biotechnology), anti-PS2 (1:100, C-20; Santa Cruz Biotechnology), anti-NCT (1:100, N-19; Santa Cruz Biotechnology), and Alexa Fluor 594 rabbit anti-goat IgG at 1:1000 (Molecular Probes, Eugene, OR, USA).

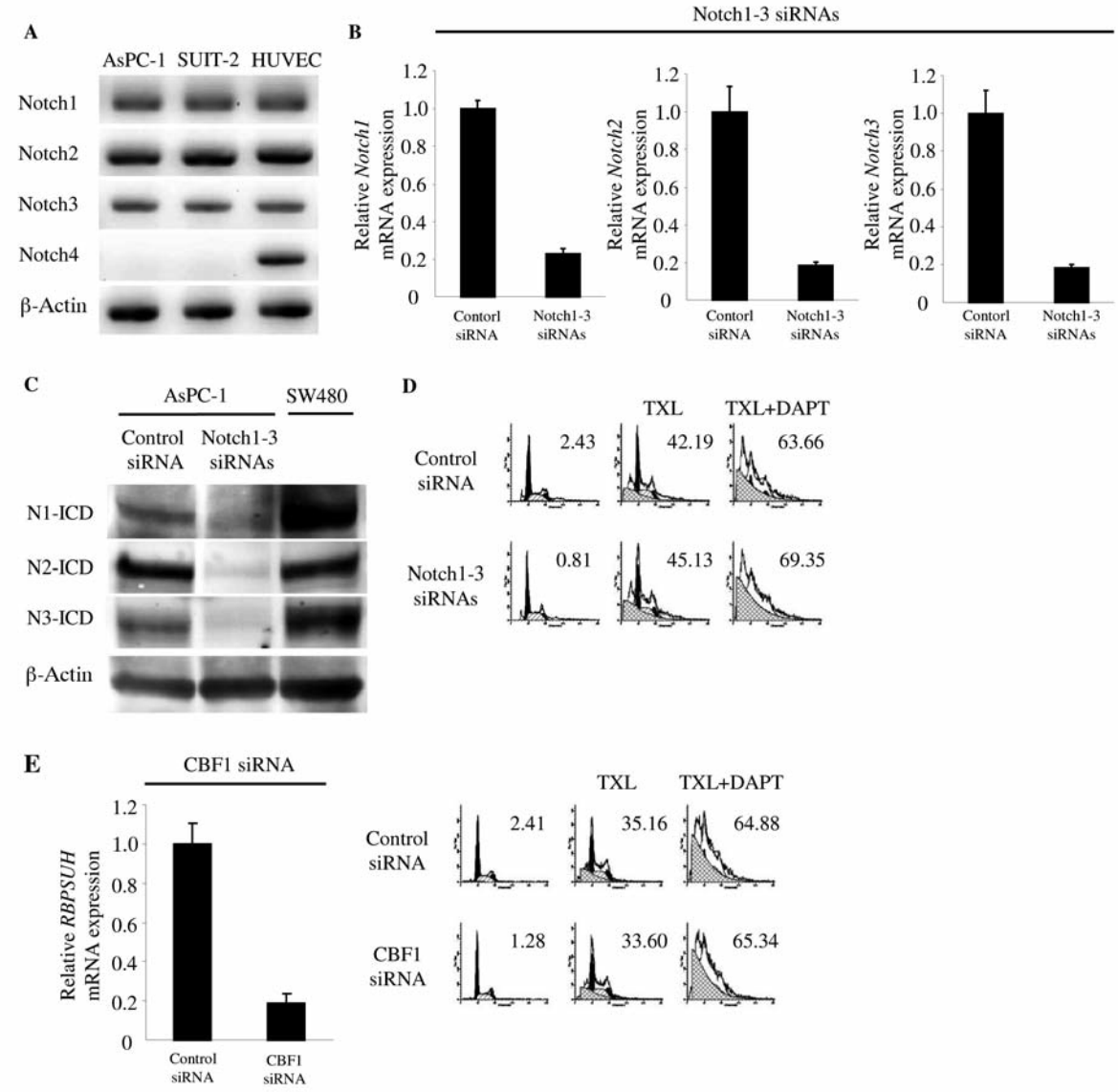

Figure 2. *Increased TXL-induced apoptosis by DAPT is independent of the Notch pathway. A: RT-PCR was used to analyse the expression of a variety of Notch receptors. HUVEC, Human umbilical vein endothelial cells. B: Real-time RT-PCR showed a simultaneous silencing of Notch1-3. C: Immunoblotting showed a significant decrease of Notch1-3-derived NICDs (N1-ICD, N2-ICD, and N3-ICD). D: Simultaneous silencing of Notch1-3 did not affect TXL-induced G_2/M accumulation or apoptosis in AsPC-1 cells. The percentage of sub-G_1 cells is indicated. E: Real-time RT-PCR showed a significant silencing of CBF1 by siRNA in AsPC-1 cells (left panel). Silencing of CBF1 did not affect TXL-induced G_2/M accumulation or apoptosis (right panels). The percentage of sub-G_1 cells is indicated. Values represent the means of triplicate experiments; bars, SD.*

Statistical analysis. Student's *t*-test was used for the statistical analyses. *P*-values of less than 0.05 were considered significant.

Results

Increase of taxane-induced apoptosis by GSIs is dependent on GS activity. DAPT at concentrations below 100 μM did not affect PDAC proliferation (data not shown). However, DAPT enhanced inhibitory proliferation by TXL and increased TXL-induced G_2/M accumulation and apoptosis (data not shown) in both AsPC-1 and SUIT-2. Similar effects by DAPT were observed in 4 out of the 5 PDAC cell lines examined (Figure 1A). Based on the preliminary data, AsPC-1 and SUIT-2 were selected as target cells that were used throughout the study. Because these effects using a combination of TXL and DAPT (TXL/DAPT) were dose and time-dependent (data not shown), the TXL concentration, DAPT concentration, and culture time were determined to be

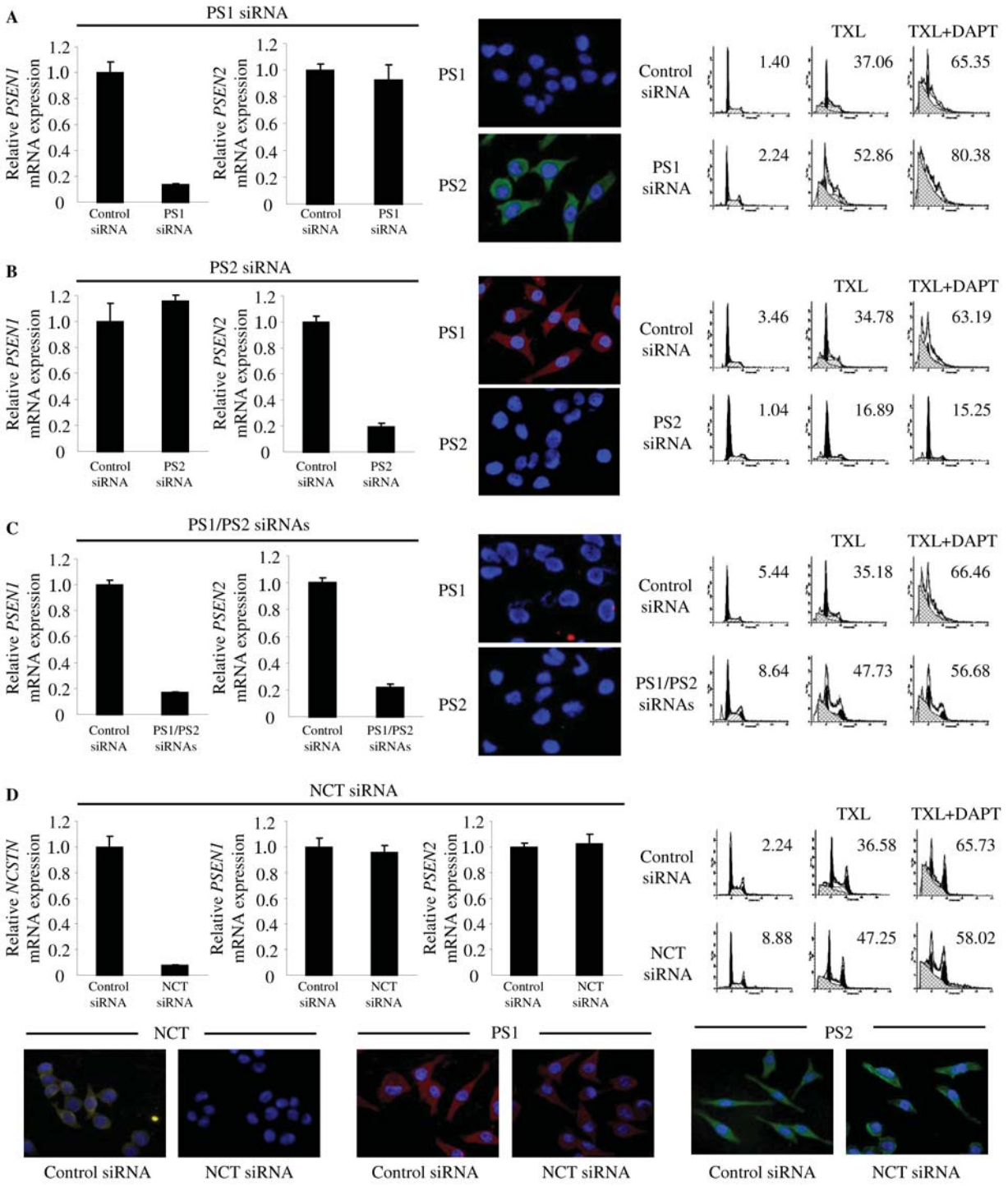

Figure 3. *Increased TXL-induced apoptosis by DAPT was observed in PS1 but not PS2 knockdown cells. A: Real-time RT-PCR showed that silencing of PS1 by siRNA significantly reduced PS1 but not PS2 mRNA levels in AsPC-1 cells (left panels). Immunofluorescence staining revealed that PS1, but not PS2, protein expression was significantly decreased (×200, middle panels). AsPC-1 cells transfected with control or PS1 siRNAs were treated with 7.5 nM TXL in the absence or presence of 25 μM DAPT for 24 h (right panels). The percentage of sub-G_1 cells is indicated. B: Silencing of PS2 by siRNA. Real-time RT-PCR (left panels). Immunofluorescence staining (×200, middle panels). Flow cytometric analysis (right panels). C: Simultaneous silencing of PS1 and PS2 by siRNAs. Real-time RT-PCR (left panels). Immunofluorescence staining (×200, middle panels). Flow cytometric analysis (right panels). D: Silencing of NCT by siRNA. Real-time RT-PCR showed that NCT silencing by siRNA did not affect the expression of PS1 or PS2 (upper left panels). Flow cytometric analysis (upper right panels). Immunofluorescence staining (×200, lower panels). Values represent the means of triplicate experiments; bars, SD.*

7.5 nM, 25 μM, and 24 h, respectively. Representative data are shown in Figure 1B. The two additional GSIs L-685,458 and compound E also increased TXL-induced apoptosis (Figure 1C). In addition, DAPT also increased TXT- and VCR-induced apoptosis (Figure 1D). DAPT did not affect apoptosis induced by other chemotherapeutic agents including GEM, 5-FU, and CDDP, which are commonly used for the treatment of patients with PDAC (Figure 1E). These results indicated that the effects of combined TXL and DAPT treatment are common for combined GSIs and AMAs, and are specific to AMAs.

Increase of TXL-induced apoptosis by DAPT is independent of the Notch pathway. When *Notch1-4* expression levels were examined by RT-PCR, the Notch receptors 1-3 were expressed in PDAC cells (Figure 2A). HUVECs were used as a positive control cell line for *Notch1-4* expression. To examine whether the Notch pathway contributes to increased TXL-induced apoptosis by DAPT, a targeted knockdown of *Notch1, Notch2*, and *Notch3* was performed. Notch1, Notch2, and Notch3 were separately knocked down using RNA interference. Transfection of siRNAs targeting *Notch1, Notch2,* and *Notch3* resulted in an 80% or greater reduction in mRNA expression (data not shown). Silencing of Notch1-3 did not affect TXL-induced apoptosis in PDAC cells (data not shown). Next, to further confirm Notch independent signalling, Notch1-3 were simultaneously silenced. Simultaneous silencing reduced the expressions of *Notch1-3* by greater than 80% (Figure 2B). In the Notch pathway, NICD translocates to the nucleus and activates the transcription of target genes (12). Therefore, to efficiently silence Notch1-3 by siRNA knockdown, it is necessary to confirm sufficient decrease of Notch1-3-derived NICDs. Simultaneous knockdown of Notch1-3 effectively reduced Notch1-3-derived NICDs (Figure 2C), but did not affect TXL or TXL/DAPT-induced apoptosis in AsPC-1 cells (Figure 2D). The SW480 human colon cancer cell line was used as a positive control. Silencing of CBF1, an essential effector of Notch signalling, did not affect TXL or TXL/DAPT-induced apoptosis (Figure 2E). These results strongly indicated Notch independent signalling in TXL/DAPT-induced apoptosis.

Silencing of PS1 but not PS2 increases TXL-induced apoptosis. To address whether PS1-GS or PS2-GS is contributing to TXL/DAPT-induced apoptosis, *PS1* and *PS2* were silenced at the mRNA level using RNA interference. Transfection of siRNA targeting *PS1* reduced the expression of *PS1* by 80% or greater, but did not affect *PS2* expression (Figure 3A; left panels). Specific silencing of PS1 was also confirmed at the protein level (Figure 3A; middle panels). As expected, silencing of PS1 increased TXL-induced apoptosis (Figure 3A; right panels). In addition, the combination of PS1-silencing and DAPT further increased the levels of

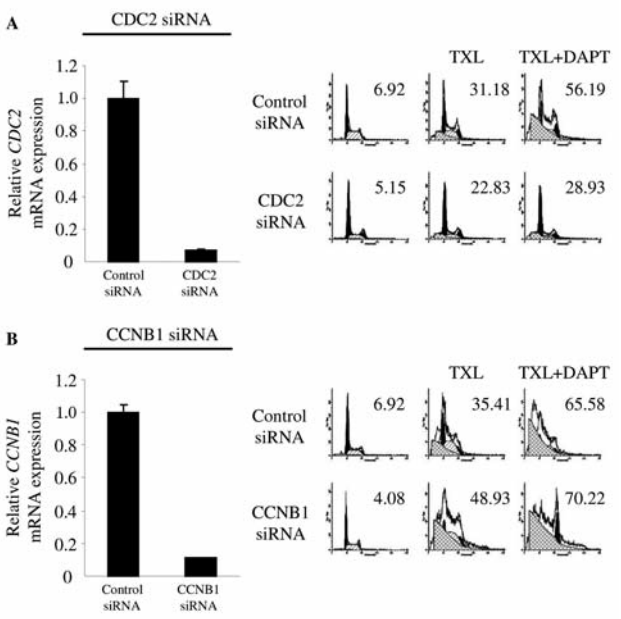

Figure 4. *Silencing of CDC2, and cyclin B1 affects TXL-induced apoptosis. A: Real-time RT-PCR showed a significant silencing of CDC2 by siRNA in AsPC-1 cells (left panel). Thereafter cells were treated with 7.5 nM TXL in the absence or presence of 25 μM DAPT for 24 h (right panels). The percentage of sub-G_1 cells is indicated. B: Silencing of cyclin B1 by siRNA. Real-time RT-PCR (left panel). Flow cytometric analysis (right panels). The percentage of sub-G_1 cells is indicated. Values represent the means of triplicate experiments; bars, SD.*

TXL-induced apoptosis. Similarly, transfection of siRNA targeting *PS2* reduced *PS2* expression by 80% or greater, but did not affect *PS1* expression (Figure 3B; left panels). Specific silencing of PS2 was also confirmed at the protein level (Figure 3B; middle panels). However, PS2 silencing suppressed TXL-induced apoptosis (Figure 3B; right panels). In addition, DAPT did not affect TXL-induced apoptosis in PS2-knockdown cells. Simultaneous silencing of PS1/PS2 effectively reduced PS1 and PS2 expression levels at the mRNA (Figure 3C; left panels) and protein levels (Figure 3C; middle panels), and significantly increased TXL-induced apoptosis. The increase was lower than the increase induced by DAPT (Figure 3C; right panels).

Next, the contribution of NCT was examined, which functions as a receptor for GS substrates or a stabiliser of GS complexes, to TXL-induced apoptosis. Transfection of siRNA targeting *NCT* reduced NCT expression at both the mRNA (Figure 3D; upper left panels) and protein levels (Figure 3D; lower panels). Silencing of NCT increased TXL-induced apoptosis (Figure 3D; upper right panels). However, this increased effect was low compared to the effect induced by DAPT. Silencing of NCT was confirmed at the protein level (Figure 3D; lower left panels). Consistent with real-time RT-PCR, silencing of NCT did not seem to affect the expression

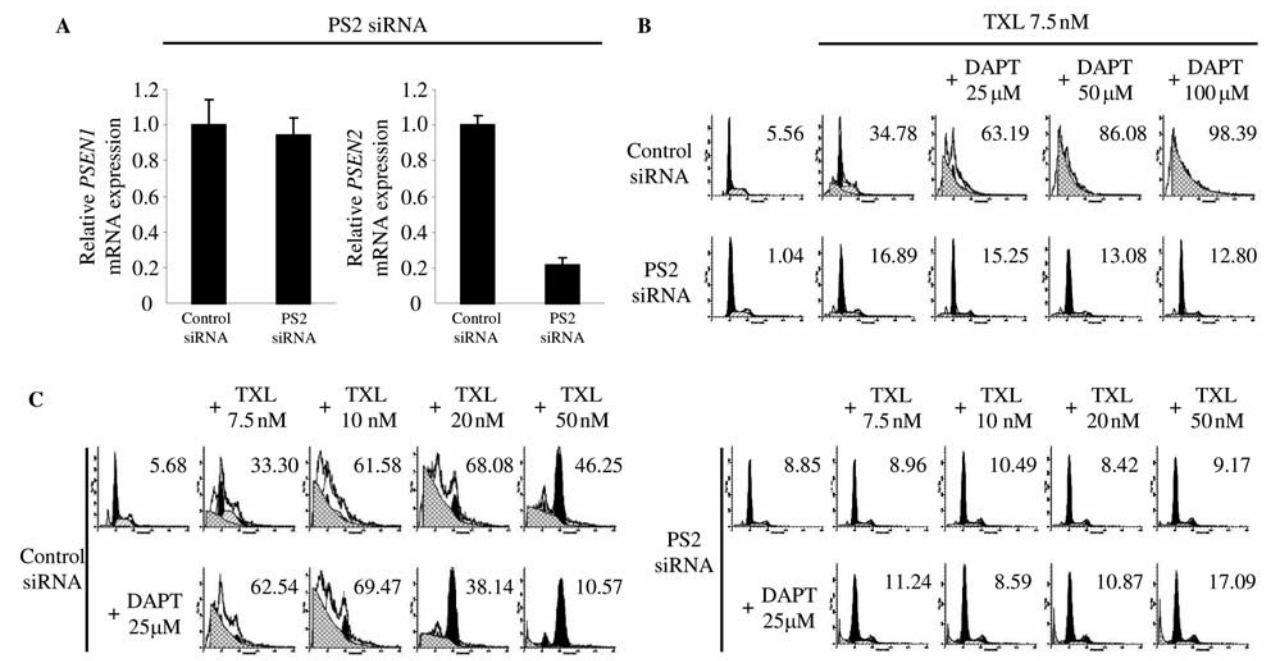

Figure 5. *A large amount of DAPT or TXL cannot restore the sensitivity of PS2-knockdown AsPC-1 cells to TXL-induced apoptosis. A: Real-time RT-PCR showed that silencing of PS2 did not affect PS1 expression in AsPC-1 cells. B: PS2-silenced AsPC-1 cells were treated with the indicated concentrations of DAPT for 24 h. The percentage of sub-G_1 cells is indicated. C: PS2-silenced AsPC-1 cells were treated with the indicated concentrations of TXL for 24 h. The percentage of sub-G_1 cells is indicated. Values represent the means of triplicate experiments; bars, SD.*

levels of PS1 (Figure 3D; lower middle panels) and PS2 (Figure 3D; lower right panels). However, staining pattern of PS2 in NCT-silencing cells seems to be relatively heterogeneous compared with that in control siRNA-transfecting cells.

Silencing of CDC2 or cyclin B1 affects TXL-induced apoptosis. Because taxanes arrest cell cycle progression in the late G_2/M phase, and cyclin B/CDC2 complex formation is crucial for G_2/M transition, it was examined whether cyclin B/CDC2 contributes to the increased effect of DAPT on TXL-induced apoptosis. Transfection of siRNA targeting *CDC2* reduced mRNA expression by 80% (Figure 4A; left panel) and decreased TXL and TXL/DAPT-induced apoptosis (Figure 4A; right panels). On the contrary, silencing of cyclin B1 (Figure 4B; left panel) increased TXL-induced apoptosis (Figure 4B; right panels). Cyclin B1 silencing, however, marginally affected TXL/DAPT-induced apoptosis.

PS2 and NCT contribute to cell proliferation in a GS-independent manner. These data show that silencing of PS2 suppressed TXL-induced apoptosis (Figure 3B). Because PS1 and PS2 compete for the shared cofactors NCT, Aph-1 and Pen2 (23), it was hypothesised that PS1-GS is the main component of this interaction, and that silencing of PS2 increases PS1 expression and consequently weakens the effect of DAPT and/or TXL. Silencing of PS2, however, did not affect the expression levels of *PS1* mRNA (Figure 5A). In addition, decreased levels of TXL-induced apoptosis in PS2-knockdown cells were not restored even with 100 μM DAPT (Figure 5B) or 50 nM/l TXL (Figure 5C) treatments. These findings suggested that silencing PS2 may abrogate the effect of TXL on the cell cycle.

Because GSIs did not affect cellular proliferation, the effect of PS silencing on cell proliferation was examined. Although silencing of PS1 did not affect proliferation, silencing of PS2 or simultaneous silencing of PS1 and PS2 almost completely inhibited proliferation (Figure 6A). Necrosis and apoptosis were not increased in PS2-knockdown or PS1/PS2-knockdown AsPC-1 cells, suggesting that cell cycle arrest is induced following PS2 silencing. DAPT did not affect the cell proliferation profiles. TXL treatment markedly decreased the proliferation of PS1-knockdown cells but did not appear to affect PS2- or PS1/PS2-knockdown cells. Combined TXL and DAPT treatment further decreased the rate of proliferation of PS1-knockdown cells, but not PS2- or PS1/PS2-knockdown cells. Silencing of NCT also decreased the cell proliferation without a significant increase in the percentages of necrotic or apoptotic cells (Figure 6B). The proliferation pattern was very similar to that observed in PS1/PS2-knockdown cells.

Silencing of PS2 but not PS1 decreases mRNA expression of cyclin D1. Because the present data indicated a contribution of PS2 to cell cycle progression, the role of PS in cell cycle

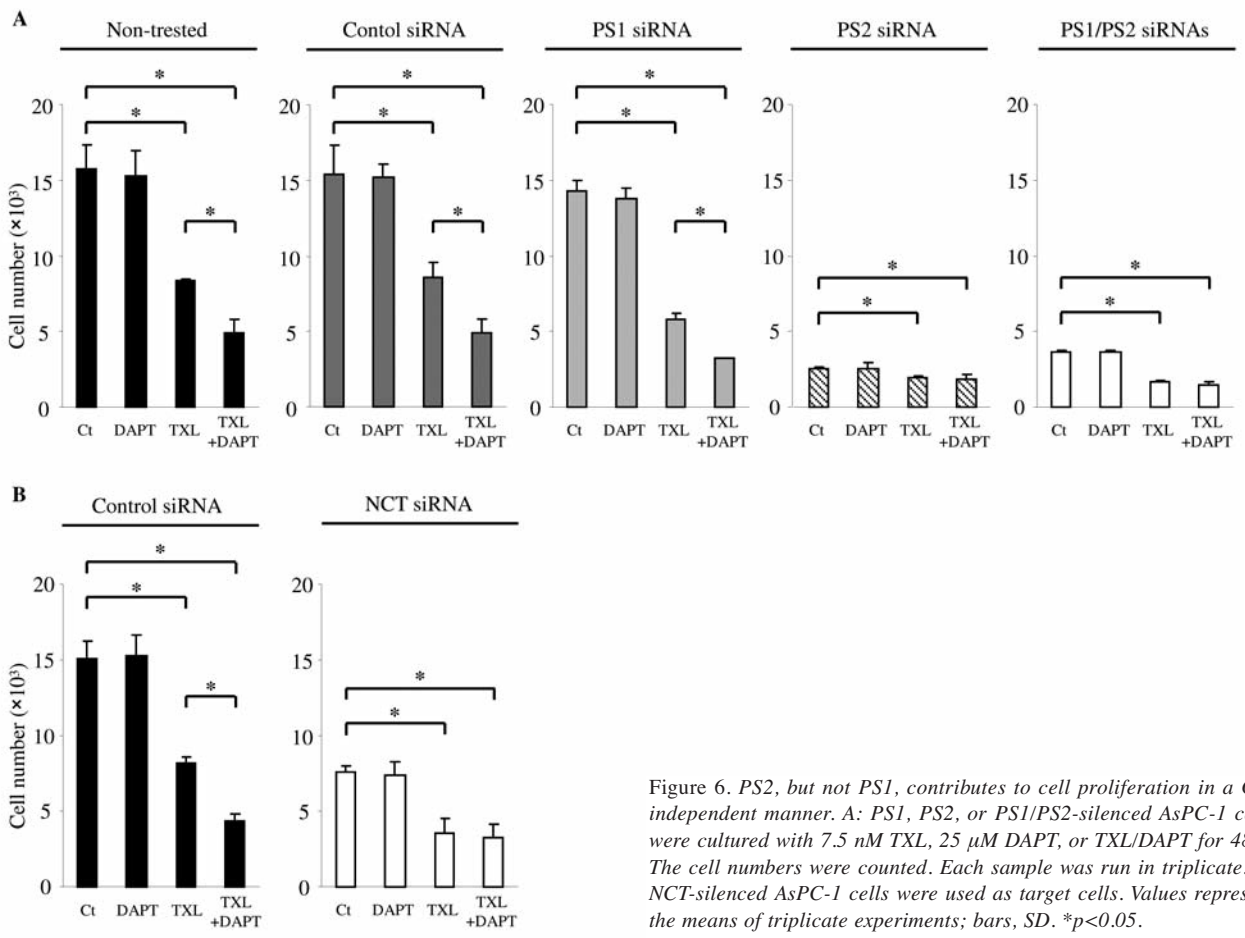

Figure 6. *PS2, but not PS1, contributes to cell proliferation in a GS-independent manner. A: PS1, PS2, or PS1/PS2-silenced AsPC-1 cells were cultured with 7.5 nM TXL, 25 μM DAPT, or TXL/DAPT for 48 h. The cell numbers were counted. Each sample was run in triplicate. B: NCT-silenced AsPC-1 cells were used as target cells. Values represent the means of triplicate experiments; bars, SD. *p<0.05.*

progression was examined. As expected, silencing of PS2 but not PS1significantly suppressed cyclin D1 expression (Figure 7A). Simultaneous silencing of PS1 and PS2 also suppressed cyclin D1 expression, but its suppression level was significantly lower compared to PS2 knockdown alone. However, silencing of PS did not affect the expression of *cyclin B1* mRNA (Figure 7B). Roscovitine, an inhibitor of cdk1, 2, and 5, inhibits cell cycle progression by preventing entry into the S and M phases. Roscovitine almost completely inhibited TXL and TXL/DAPT-induced apoptosis and cell proliferation (Figure 7C). Taken together, these data indicated that silencing of PS2 strongly suppresses the cell cycle progression in a GS-independent manner.

Discussion

This study reported that PS-GS plays a crucial role in the resistance of PDAC to taxanes, and GSIs may be therefore enhance sensitivity to taxanes. This effect of GSIs is independent of Notch signalling. In addition, this study showed for the first time that PS2 acts as an accelerator and regulates cell cycle progression independently of GS activity. Thus, it is hypothesised that PS regulates the response of PDAC against AMAs through both GS-dependent and GS-independent mechanisms.

Increasing evidence suggests that GS complexes have both GS-dependent and -independent functions (9). For example, PS has also been reported to possess GS-independent functions, such as the regulation of β-catenin/cyclin D (24). Therefore, it was first examined whether this effect of GSIs is dependent on GS. Because three different GSIs, which specifically inhibit PS-GS activity, showed similar effects on taxane-induced apoptosis, it was concluded that this effect was dependent on PS-GS. It is supposed that each GS complex contains only one PS subunit, PS1 or PS2, and that the substrate-specificity of PS1 and PS2 is different (17). Therefore, this study examined which PS subunits were involved in the GSI-induced effects. The present study showed that silencing of PS1, but not PS2, enhanced taxane-induced apoptosis. Surprisingly, the silencing of PS2 reduced the effect of TXL- and TXL/DAPT-induced apoptosis. Based on these observations, it was supposed at first that PS1-GS

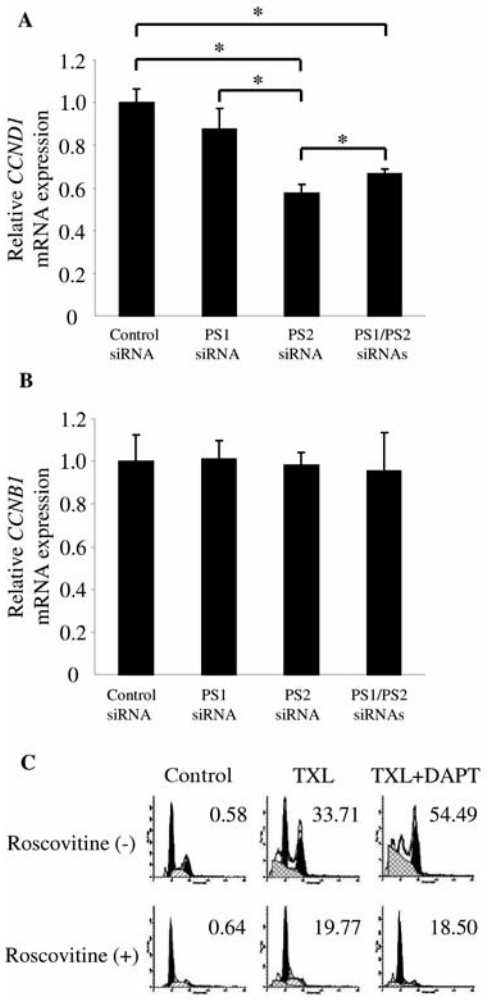

Figure 7. *Silencing of PS2, but not PS1, decreases the expression of cyclin D1. A: Real-time RT-PCR demonstrated that silencing of PS2 or PS1/PS2 decreased cyclin D1 mRNA expression. B: Real-time RT-PCR revealed that silencing of PS1, PS2 or PS1/PS2 did not affect cyclin B1 mRNA expression. C: AsPC-1 cells were treated with drugs (7.5 nMl TXL, 25 μM DAPT, 25 μM roscovitine) for 24 h. The percentage of sub-G_1 cells is indicated. Values represent the means of triplicate experiments; bars, SD. *p<0.05.*

Table II. *Similar effects of GSIs on TXL-induced apoptosis in colon cancer cells and PDAC.*

	Colon cancer cells*	PDAC cells**
1. GS activity-dependent		
TXL	+	+
TXL/DAPT	+++	+++
TXL/L-685,458	+++	+++
TXL/Compound E	+++	+++
2. AMD-dependent		
TXT	+	+
TXT/DAPT	+++	+++
Vincristine	+	+
Vincristine/DAPT	+++	+++
5-FU	+	+
5-FU/DAPT	+	+
Gemcitabine	Not tested	+
Gemcitabine/DAPT	Not tested	+
Cisplatin	+	+
Cisplatin/DAPT	+	+
Camptothecin	+	Not tested
Camptothecin/DAPT	+	Not tested
3. Notch-independent		
TXL/Notch1(–)	+	+
TXL/Notch1(–)/DAPT	+++	+++
TXL/Notch2(–)	+	+
TXL/Notch2(–)/DAPT	+++	+++
TXL/Notch3(–)	+	+
TXL/Notch3(–)/DAPT	+++	+++
TXL/Notch1(–)/Notch2(–)/Notch3(–)	Not tested	+
TXL/Notch1(–)/Notch2(–)/Notch3(–)/DAPT	Not tested	+++
TXL/CBF1(–)	+	+
TXL/CBF1(–)/DAPT	+++	+++
TXL/NICD(+)	+	Not tested
TXL/NICD(+)/DAPT	+++	Not tested
4. Cell cycle-dependent		
TXL/Roscovitine	–	–
TXL/DAPT/Roscovitine	–	–
TXL/CDC2(–)	–	–
TXL/cyclinB1(–)	++	++
5. Caspase-independent		
TXL/zVAD-fmk	+	+
TXL/DAPT/zVAD-fmk	+++	+++

*SW480 cells, **AsPC-1 cells + % apoptosis at 7.5 nm TXL (control % apoptosis); ++ moderate increase over control % apoptosis; +++ marked increase over control % apoptosis; – significant decrease compared to control % apoptosis.

decreased the sensitivity of PDAC to taxanes, and that PS2-GS may suppress this function of PS1-GS. However, this hypothesis was not correct because the data also suggested the possibility that PS2 silencing suppresses TXL-induced apoptosis by inhibiting cell cycle progression in a GS-independent manner. Therefore, it is hypothesised that both PS1-GS and PS2-GS are involved in the resistance to taxanes, because the combination of PS1 silencing and DAPT further increased TXL-induced apoptosis.

There are several potential mechanisms by which PS-GS contributes to the resistance of PDAC to taxanes. Cancer cells must possess several protective mechanisms for disabling the G_1 or G_2 checkpoint mechanisms because they have already acquired several genetic mutations. It is recognised that taxanes induce the accumulation of cells in the G_2/M phase and result in apoptosis by increasing microtubule polymerisation (19). The higher the TXL concentration, the higher are the resulting levels of G_2/M accumulation and apoptosis at the early stage (data not shown). Similarly, DAPT accelerated the onset of TXL-induced apoptosis (data not shown). This finding suggests

that the effects of PS-GS and TXL on the cell cycle are closely linked. Because taxanes block cell cycle progression in the late G_2/M phase, PS-GS may also be involved in the G_2/M phase. A previous study demonstrated that TXL increases CDC2/cyclin B activity, required for the G2/M transition, in a dose-dependent manner, and DAPT further increased this activity in colon cancer cells (2). Taken together, it is hypothesised that TXL accelerates both the progression from G_2 phase to M phase and also simultaneously suppresses the progression from metaphase to anaphase. Furthermore, it is likely that PS-GS acts as a suppressor against these taxane functions. This hypothesis is supported by the data of the current study. TXL-induced apoptosis was reduced by silencing CDC2. It is known that CDC2 is required for progression from S to G_2. Thus, silencing CDC2 prevents entry from S phase to G_2 phase, and consequently reduces G_2/M accumulation. However, silencing of cyclin B suppresses progression from G_2 to M and consequently increases G_2/M accumulation. GSIs may increase the levels of apoptosis by increasing G_2/M accumulation and/or mitotic arrest. Several studies have suggested the possibility of cell cycle regulation, including G_0/G_1 and G_2/M arrest, by GS in various cancer cell types (25).

The next question is which substrates are targets for PS-GS. The *Notch* gene was examined, because it has been shown that Notch1 is overexpressed in PDAC (11). In addition, Notch plays an important role in maintaining the undifferentiated, proliferative state of crypt progenitors in mouse intestines (26); consistent with this, GSIs exhibit gastrointestinal toxicity (27). Because the present study was conducted to contribute to the knowledge used by physicians, it is important to determine whether the effect of GSIs is Notch-dependent. The present data strongly indicated Notch-independency, as follows: firstly, the simultaneous silencing of Notch 1-3 significantly reduced the expression of NICDs, but did not affect TXL- or TXL/DAPT-induced apoptosis. Secondly, the silencing of CBF1, an essential effector of Notch signalling, did not affect TXL- or TXL/DAPT-induced apoptosis. It is noteworthy that the effects of DAPT on TXL-induced apoptosis in PDAC were consistent with those in colon cancer (2) (Table II). Previously published data concerning colon cancer also suggested GSI-induced Notch-independent effects; the overexpression of NICD in colon cancer cells did not affect DAPT effects (data not shown). Taken together, it is concluded that the effects induced by GSIs are independent of Notch. Potential target substrates were examined intensively using known candidate molecules, including E-cadherin, CD44, and ephrin-B1 (data not shown). However, it was not possible to definitively identify those substrates which are targets for PS-GS, which will be examined in future studies.

The present study showed that PS contributes to cell proliferation in a GS-independent manner. A possibility of modulation of the cell cycle by PS has been suggested (25, 28-30). For example, it has been shown that overexpression of PS induces G_1 arrest (28), and that loss of PS in peripheral tissues leads to the activation of cyclin D1 and hyperproliferation (29). It has also been indicated that neurons harbouring the PS1 mutation show cyclin D1 up-regulation and an abnormal neuronal cell cycle (30). Recent reports also revealed a possibility that the neuronal cell cycle is mediated by a PS1 hydrophilic loop in a GS-independent manner (25). These findings indicated that PS, and PS1 in particular, is a negative regulator of cyclin D1 in peripheral tissues. However, the present data showed that knockdown of PS2 but not PS1 induces cyclin D1 down-regulation and suppresses the proliferation of PDAC cells. These findings indicated that PS2 regulates the cell cycle and acts as an accelerator. The current data also showed that knockdown of PS1 but not PS2 increased *Myc* mRNA expression (data not shown). In addition, because the degree of cyclin D1 down-regulation and proliferation suppression in PS1/PS2-knockdown cells are low compared to PS2-silenced cells, one cannot rule out the possibility that PS1 acts as a negative regulator in cell cycle progression (28, 29). It is proposed that PS2 and PS1 have accelerating and suppressing roles in cell cycle progression, respectively. In the presence of wild-type PS2, the suppressive function of PS1 may be phenotypically concealed due to the strong accelerating function of PS2. Because GSIs did not affect both cell cycle progression and cell proliferation, this effect of PS is independent of GS. Taken together, it is concluded that GS complexes regulate the response of PDAC against AMAs through both GS-dependent and GS-independent mechanisms. However, the molecular mechanism by which PS controls the cell cycle progression is still unknown.

Acknowledgements

The Notch2 monoclonal antibody developed by Dr. Spyros Artavanis-Tsakonas was obtained from the University of Iowa Development Hybridoma Studies bank.

We thank Dr. Rapahel Kopan (Washington University) for generously providing the vectors and Kaori Nomiyama for skillful technical assistance. This study was supported by General Scientific Research Grants (20390361, 21390363, and 19390337) from the Ministry of Education, Culture, Sports, Science, and Technology of Japan.

References

1 Jemal A, Siegel R, Ward E, Hao Y, Xu J and Thun MJ: Cancer statistics, 2009. CA Cancer J Clin *59*: 225-249, 2009.

2 Akiyoshi T, Nakamura M, Yanai K, Nagai S, Wada J, Koga K, Nakashima H, Sato N, Tanaka M and Katano M: Gamma-secretase inhibitors enhance taxane-induced mitotic arrest and apoptosis in colon cancer cells. Gastroenterology *134*: 131-144, 2008.

3 Sato T, Diehl TS, Narayanan S, Funamoto S, Ihara Y, De Strooper B, Steiner H, Haass C and Wolfe MS: Active gamma-secretase complexes contain only one of each component. J Biol Chem *282*: 33985-33993, 2007.

4 Shirotani K, Edbauer D, Prokop S, Haass C and Steiner H: Identification of distinct gamma-secretase complexes with different APH-1 variants. J Biol Chem *279*: 41340-41345, 2004.
5 Dries DR, Shah S, Han YH, Yu C, Yu S, Shearman MS and Yu G: Glu-333 of nicastrin directly participates in gamma-secretase activity. J Biol Chem *284*: 29714-29724, 2009.
6 Takasugi N, Tomita T, Hayashi I, Tsuruoka M, Niimura M, Takahashi Y, Thinakaran G and Iwatsubo T: The role of presenilin cofactors in the gamma-secretase complex. Nature *422*: 438-441, 2003.
7 Donoviel DB, Hadjantonakis AK, Ikeda M, Zheng H, Hyslop PS and Bernstein A: Mice lacking both presenilin genes exhibit early embryonic patterning defects. Genes Dev *13*: 2801-2810, 1999.
8 Shen J, Bronson RT, Chen DF, Xia W, Selkoe DJ and Tonegawa S: Skeletal and CNS defects in Presenilin-1-deficient mice. Cell *89*: 629-639, 1997.
9 Parks AL and Curtis D: Presenilin diversifies its portfolio. Trends Genet *23*: 140-150, 2007.
10 Wakabayashi T and De Strooper B: Presenilins: members of the gamma-secretase quartets, but part-time soloists too. Physiology (Bethesda) *23*: 194-204, 2008.
11 Wang Z, Zhang Y, Li Y, Banerjee S, Liao J and Sarkar FH: Down-regulation of Notch-1 contributes to cell growth inhibition and apoptosis in pancreatic cancer cells. Mol Cancer Ther *5*: 483-493, 2006.
12 De Strooper B, Annaert W, Cupers P, Saftig P, Craessaerts K, Mumm JS, Schroeter EH, Schrijvers V, Wolfe MS, Ray WJ, Goate A and Kopan R: A presenilin-1-dependent gamma-secretase-like protease mediates release of Notch intracellular domain. Nature *398*: 518-522, 1999.
13 Iso T, Kedes L and Hamamori Y: HES and HERP families: multiple effectors of the Notch signaling pathway. J Cell Physiol *194*: 237-255, 2003.
14 Rizzo P, Osipo C, Foreman K, Golde T, Osborne B and Miele L: Rational targeting of Notch signaling in cancer. Oncogene *27*: 5124-5131, 2008.
15 Kreft AF, Martone R and Porte A: Recent advances in the identification of gamma-secretase inhibitors to clinically test the Abeta oligomer hypothesis of Alzheimer's disease. J Med Chem *52*: 6169-6188, 2009.
16 Fuwa H, Takahashi Y, Konno Y, Watanabe N, Miyashita H, Sasaki M, Natsugari H, Kan T, Fukuyama T, Tomita T and Iwatsubo T: Divergent synthesis of multifunctional molecular probes to elucidate the enzyme specificity of dipeptidic gamma-secretase inhibitors. ACS Chem Biol *2*: 408-418, 2007.
17 Lai MT, Chen E, Crouthamel MC, DiMuzio-Mower J, Xu M, Huang Q, Price E, Register RB, Shi XP, Donoviel DB, Bernstein A, Hazuda D, Gardell SJ and Li YM: Presenilin-1 and presenilin-2 exhibit distinct yet overlapping gamma-secretase activities. J Biol Chem *278*: 22475-22481, 2003.
18 Jordan MA and Wilson L: Microtubules as a target for anticancer drugs. Nat Rev Cancer *4*: 253-265, 2004.
19 Fuchs DA and Johnson RK: Cytologic evidence that paclitaxel, an antineoplastic agent from *Taxus brevifoliaz* acts as a mitotic spindle poison. Cancer Treat Rep *62*: 1219-1222, 1978.
20 Kastan MB and Bartek J: Cell-cycle checkpoints and cancer. Nature *432*: 316-323, 2004.
21 Stark GR and Taylor WR: Control of the G_2/M transition. Mol Biotechnol *32*: 227-248, 2006.
22 Fan W: Possible mechanisms of paclitaxel-induced apoptosis. Biochem Pharmacol *57*: 1215-1221, 1999.
23 Placanica L, Tarassishin L, Yang G, Peethumnongsin E, Kim SH, Zheng H, Sisodia SS and Li YM: Pen2 and presenilin-1 modulate the dynamic equilibrium of presenilin-1 and presenilin-2 gamma-secretase complexes. J Biol Chem *284*: 2967-2977, 2009.
24 Soriano S, Kang DE, Fu M, Pestell R, Chevallier N, Zheng H and Koo EH: Presenilin 1 negatively regulates beta-catenin/T cell factor/lymphoid enhancer factor-1 signaling independently of beta-amyloid precursor protein and notch processing. J Cell Biol *152*: 785-794, 2001.
25 Kallhoff-Munoz V, Hu L, Chen X, Pautler RG and Zheng H: Genetic dissection of gamma-secretase-dependent and -independent functions of presenilin in regulating neuronal cell cycle and cell death. J Neurosci *28*: 11421-11431, 2008.
26 Fre S, Huyghe M, Mourikis P, Robine S, Louvard D and Artavanis-Tsakonas S: Notch signals control the fate of immature progenitor cells in the intestine. Nature *435*: 964-968, 2005.
27 Wong GT, Manfra D, Poulet FM, Zhang Q, Josien H, Bara T, Engstrom L, Pinzon-Ortiz M, Fine JS, Lee HJ, Zhang L, Higgins GA and Parker EM: Chronic treatment with the gamma-secretase inhibitor LY-411,575 inhibits beta-amyloid peptide production and alters lymphopoiesis and intestinal cell differentiation. J Biol Chem *279*: 12876-12882, 2004.
28 Janicki SM and Monteiro MJ: Presenilin overexpression arrests cells in the G1 phase of the cell cycle. Arrest potentiated by the Alzheimer's disease PS2(N141I) mutant. Am J Pathol *155*: 135-144, 1999.
29 Xia X, Qian S, Soriano S, Wu Y, Fletcher AM, Wang XJ, Koo EH, Wu X and Zheng H: Loss of presenilin 1 is associated with enhanced beta-catenin signaling and skin tumorigenesis. Proc Natl Acad Sci USA *98*: 10863-10868, 2001.
30 Malik B, Currais A, Andres A, Towlson C, Pitsi D, Nunes A, Niblock M, Cooper J, Hortobagyi T and Soriano S: Loss of neuronal cell cycle control as a mechanism of neurodegeneration in the presenilin-1 Alzheimer's disease brain. Cell Cycle *7*: 637-646, 2008.

Received October 4, 2010
Revised November 5, 2010
Accepted November 8, 2010